Histol Histopathol (2020) 35: 269-278

http://www.hh.um.es

Histology and Histopathology

From Cell Biology to Tissue Engineering

Latexin expression correlated with mineralization of articular cartilage during progression of post-traumatic osteoarthritis in a rat model

América Martínez-Calleja[1], Raymundo Cruz[1], Magdalena Miranda-Sánchez[1], Rogelio Fragoso-Soriano[2], Marco A. Vega López[1] and Juan B. Kouri[1]

[1]Department of Infectomic and Molecular Pathogenesis and [2]Department of Physics, Center for Research and Advanced Studies of the Polytechnic National Institute (CINVESTAV-IPN), Mexico City, Mexico

Summary. As latexin has been linked with chondrocyte hypertrophic differentiation it is possible that this protein may also be involved in the mineralization of cartilage in OA. Therefore, we correlated latexin expression with the mineralization marker, alkaline phosphatase and determined the mineral deposition in the articular cartilage by analyzing the Ca/P ratio and the collagen fibrils pattern, during the progression of post-traumatic OA in a rat model. OA was induced by medial meniscectomy and post-surgery exercise for 5, 10, 20 and 45 days. Protein expression in articular cartilage was evaluated by immunofluorescence, histochemistry and Western blot. Minerals and structure of collagen fibrils in the superficial zone of cartilage were analyzed by energy dispersive X-ray spectroscopy (EDX) and atomic force microscopy (AFM) respectively. Protein expression analysis showed time-dependent up-regulation of latexin during OA progression. In the cartilage, latexin expression correlated with the expression and activity of alkaline phosphatase. EDX of the superficial zone of cartilage showed a Ca/P ratio closer to theoretical values for basic calcium phosphate minerals. The presence of minerals was also analyzed indirectly with AFM, as the collagen fibril pattern was less evident in the mineralized tissue. Latexin is expressed in articular cartilage from the early stages of post-traumatic OA; however, minerals were detected after latexin expression was up-regulated, indicating that its activity precedes and remains during the pathological mineralization of cartilage. Thus, our results contribute to the identification of molecules involved in the mineralization of articular chondrocytes.

Key words: Osteoarthritis, Chondrocyte hypertrophy, Mineralization, Articular cartilage, Latexin

Offprint requests to: Marco A. Vega López or Raymundo Cruz, Departamento de Infectómica y Patogénesis Molecular, Centro de Investigación y de Estudios Avanzados del Instituto Politécnico Nacional (CINVESTAV-IPN), Av. IPN. 2508, San Pedro Zacatenco, Ciudad de México, 07360, México. e-mail: mavega@cinvestav.mx or jrcruz@cinvestav.mx

DOI: 10.14670/HH-18-151

Introduction

Osteoarthritis (OA) is a chronic and degenerative joint disorder characterized by articular cartilage degradation, mild synovitis, and peri-articular/subchondral bone alterations (Goldring and Goldring, 2010).

In addition to the progressive degeneration of articular cartilage during OA pathogenesis, abnormal mineral deposition in the extracellular matrix (ECM) has been reported (Fuerst, 2014). Two kinds of calcium-containing minerals have been identified in the synovial fluid, synovium, and articular cartilage in patients with OA: calcium pyrophosphate dihydrate (CPPD) and basic calcium phosphates (BCPs) such as carbonate-substituted hydroxyapatite (HA), tricalcium phosphate (TCP), and octacalcium phosphate (OCP) (Fuerst et al., 2009; Frallonardo et al., 2016; Corr et al., 2017). The origin and pathogenic role of minerals in joints are still unclear, but chondrocytes undergoing abnormal mineralization processes express a variety of proteins similar to those expressed by hypertrophic chondrocytes

during endochondral ossification, including collagen X, MMP-13, and alkaline phosphatase (Velasquillo et al., 2007; Fuerst, 2014). Alkaline phosphatase (ALP) has increased activity in the cartilage of end-stage OA patients, contributing to the mineralization process (Kouri et al., 2000; Yamaguchi et al., 2014) as it hydrolyzes organic phosphate compounds to increase the inorganic phosphate concentration, thus facilitating the deposition of calcium phosphate in the form of HA (Golub, 2009; Orimo, 2010).

In our search for new biomarkers of OA pathogenesis, proteomic approaches showed the expression of latexin (Lxn) in articular cartilage from healthy rats (Perez et al., 2010), with expression levels being up-regulated during OA progression (Parra-Torres et al., 2014). However, the specific role of Lxn in the pathogenesis of this disease is not yet known. Lxn is an inhibitor of carboxypeptidase A (CPA) in mammals (Liang and Van Zant, 2008; Arimatsu et al., 2009) where it modulates the apoptosis and senescence of cells (Liang and Van Zant, 2008). However, its sequence is unrelated to any other reported carboxipeptidase inhibitors, but shows significant homology with the tumor suppressor, Tazarotene-Induced Gene 1 (TIG1) (Aagaard et al., 2005) and with the chicken Ovocalycin-32 (OCX-32), a protein associated with mineral deposition in the eggshell (Hincke et al., 2003). Despite important molecular characterization, the mechanism of action has remained elusive since Lxn appears to be able to function independently of its classical CPA inhibitory activity (Ni et al., 2014). Thus, gene expression profiling showed Lxn expression during bone morphogenetic protein-2 (BMP-2)-mediated osteoblast differentiation, suggesting a new role for this protein in the bone microenvironment (Balint et al., 2003). Lxn has also been associated with chondrocyte differentiation, as it is expressed in prehypertrophic chondrocytes during skeletogenesis and bone fracture repair (Kadouchi et al., 2009), where it is also up-regulated, via sox-9, by BMP-2, a protein with a primary role in endochondral ossification (Yu et al., 2010). However, further functional studies are still necessary to elucidate the precise molecular mechanism on the role of Lxn in chondrocyte differentiation/mineralization process.

As Lxn is involved in BMP-2-induced chondrocyte hypertrophic differentiation, it is possible that this protein may also be involved—directly or indirectly—in the mineralization of cartilage in OA. Therefore, the aim of this research was to investigate the correlation between Lxn expression and the mineralization biomarker ALP and to analyze the mineral deposition in the articular cartilage by the Ca/P molar ratio and the collagen fibrils pattern, during the progression of post-traumatic OA.

Materials and methods

Animals and experimental groups

Male Wistar rats (6-7 weeks old) were housed in a 12-h light/dark schedule and allowed free access to food and water. All surgical procedures were carried out in anesthetized rats with an intraperitoneal injection of ketamine/xylazine solution. Animals were euthanized by CO_2 inhalation, and cartilage samples were removed under aseptic conditions.

For histochemistry and immunofluorescence analyses we used 9 rats per experimental group (108 rats in total). For atomic force microscopy (AFM) and energy-dispersive X-ray (EDX) studies we used 3 rats per experimental group (15 rats for each technique), and for Western blot studies we used 30 rats per experimental group (560 rats, because we pooled the cartilage from 10 condyles to obtain sufficient protein sample per experimental group and because we ran distinct experimental repetitions (n) for groups, that were properly indicated when required).

The surgical procedure to induce OA has been reported in detail elsewhere (Lozoya and Flores, 2000) and involves a meniscectomy of the medial meniscus from the right knee (OA groups). As a control for the acute synovitis resulting from the surgery, we included sham-operated rats. We also included a control group of normal rats without surgery or high-impact exercise but following the same time sequences as the sham and OA rats. For AFM and EDX analyses, we compared the mineral deposition indicators in OA cartilage with those in healthy cartilage from randomly picked normal rats.

The exercise regimen has been described in detail elsewhere (Rojas-Ortega et al., 2015) and began 2 days after the surgery, for 5, 10, 20 and 45 days, hereafter called days post-surgery. Euthanasia was performed 24 hours after the last day of exercise for each experimental group.

All procedures for animal care and use were approved by our institutional *ad hoc* committee and follow the Mexican official regulatory guideline NOM-062-ZOO-1999.

Tissue samples

We obtained the medial femoral condyles from the right knee for all studies. For histological studies and AFM, condyles were fixed for 12 h at 4°C in 4% paraformaldehyde in PBS, pH 7.2. After 3 washes with PBS, samples were incubated in sucrose 10% in PBS, pH 7.2 for 12 h at 4°C, then embedded in tissue freezing medium (Leica microsystems, Wetzlar, Germany) and frozen at -20°C. To analyze *in situ* ALP activity, condyles were frozen at -20°C and then cryosectioned without fixation. For EDX analyses, condyles were sectioned in half in the sagittal plane, fixed in formalin 10% for 3 h and then processed for carbon coating. For the Western blot, we obtained the articular cartilage from each experimental group and then immediately froze and stored them at -80°C until processing to extract the proteins.

For analysis we divided the articular cartilage in three zones: Superficial (SZ), Middle (MZ) and Deep

(DZ). In the OA cartilage some chondrocyte layers were reduced or lost; therefore, we performed the analysis only where the three zones were still present; chondrocytes of the calcified cartilage were not included in the analysis.

Western blot

Pooled cartilage samples (approximately 0.2 g) were homogenized in 500 μL lysis buffer [25 mM Tris-HCl, pH 7.6, 150 mM NaCl, 0.2 mM EDTA, 0.5 mM dithiothreitol, 1% Triton X-100 and enzyme inhibitors cocktail (Complete, Roche Applied Science, Manheim, Germany)] and then clarified by centrifugation for 5 min at 10,000 x g. SDS-PAGE was performed using 15% gels and 40 µg protein per gel lane. Nitrocellulose membranes were blocked with 5% nonfat dry milk and 0.5% BSA in Tris-buffered saline, pH 7.5, containing 0.1% Tween 20 (TBS-T) for 2 h at 37°C and then incubated overnight at 4°C with either goat anti-Lxn antibody (1:300, sc-47089, Santa Cruz Biotechnology, Santa Cruz, CA, USA) or rabbit anti-ALP antibody (1:800; Sc-30203, Santa Cruz Biotechnology). The immunoreactions were observed after 1 h of incubation with horseradish peroxidase-labeled anti-goat or anti-rabbit secondary antibodies (1:90000, and 1:80000 respectively, Jackson Immunoresearch Inc. West Grove, PA, USA), using the chemiluminescence ECL Plus Western blotting detection system. β-actin expression (1:200, sc-1616, Santa Cruz Biotechnology) was used as an internal control for each experimental group. The protein bands (Lxn 29 kDa, ALP 80 kDa and actin 43 kDa) were quantified by densitometry with Image J software (http://imagej.nih.gov/ij/). Protein expression values are shown as the ratio of Lxn or ALP/actin. Data are shown as mean ± standard deviation, and statistical significance is represented as $p<0.01$(**) or $p<0.001$(***) when OA groups are compared to their normal- and sham-paired groups. Comparisons between normal groups at 5 days and at 10, 20, and 45 days post-surgery and between sham groups at 5 days and at 10, 20, and 45 days post-surgery are represented as $p<0.001$($^{\&\&\&}$) and $p<0.001$($^{+++}$), respectively. The number of independent repetitions (n) is indicated properly in the figure legends.

Immunofluorescence

Frozen condyles were cryosectioned in the sagittal plane of the tissue (Cryostat Leica CM 1100, Leica microsystems) to obtain 7-µm thick slices, which were mounted on gelatin-coated slides. The sections were hydrated for 15 min in PBS and permeabilized with 0.2% Tween-20 in PBS for 10 min at room temperature. They were then pre-incubated with 0.2% IgG-free BSA for 20 min at room temperature. To identify the proteins, the samples were incubated overnight at 4°C with goat anti-Lxn antibody (1:40, sc-47089, Santa Cruz Biotechnology), followed by incubation with fluorescein isothiocyanate (FITC)-tagged donkey anti-goat IgG (1:50, Jackson Immunoresearch Inc.) for 1 h at room temperature. Cartilage samples with the corresponding primary antibodies replaced with non-immune goat serum (1:40) were used as negative controls. Nuclei were counterstained with propidium iodide (10 µg/mL, Sigma-Aldrich Inc., St. Louis, MO, USA), for 5 min and mounted with vectashield (Vector laboratories, Burlingame, CA, USA).

Fluorescence analyses were performed with an inverted Confocal microscope (TCS-SP5-DMI6000B, Leica microsystems), using a 40X plan neofluar oil immersion lens. Fluorochromes were excited with 488 nm argon laser and 543 nm helium-neon laser lines. Images from three different fields of each section (3 sections per slide) were captured and processed using the LAS AF lite Confocal software (Leica microsystems). From the recorded green (FITC) channel images, we obtained the total number of pixels per area (μm^2) of nine microscopic fields per animal across the three zones of cartilage. Data are shown as mean ± standard deviation, and statistical significance is represented as $p<0.05$(*), $p<0.01$(**), or $p<0.001$(***) when OA groups are compared to their normal- and sham-paired groups. Comparisons between normal groups at 5 days and at 10, 20, and 45 days post-surgery and between sham groups at 5 days and at 10, 20, and 45 days post-surgery are represented as $p<0.05$($^{\&}$) and $p<0.01$($^{\&\&}$) or $p<0.05$($^{+}$) and $p<0.01$($^{++}$), respectively. Nine rats per experimental group were used (n=9).

Alkaline phosphatase activity

Condyles were cryosectioned to obtain 7-μm thick slices and mounted on gelatin-coated slides. Slices were immediately used to measure alkaline phosphatase activity with a commercial kit (86R, Sigma-Aldrich Inc.), following the manufacturer's instructions with minor modifications. After incubation with the ALP substrate for 1 h at 37°C, tissue slices were washed with deionized water and then air-dried. The cells that were positive for ALP activity developed a red/light purple color. As negative controls, the cartilage samples were boiled to deactivate the enzyme. Slices were mounted with Poly-Mount resin (Polysciences, Inc. Warrington, PA, USA). Images from three different fields of each section (3 sections per slide) were captured with a digital camera (DFC320, Leica microsystems) with LAS image manager software (Leica microsystems) coupled to the microscope (DMLS, Leica microsystems), using a 40X Plan lens. We scored nine microscopic fields per animal and counted the positive cells in the recorded images. The total count of chondrocytes per zone was considered 100%. Data are shown as mean ± standard deviation, and statistical significance is represented as $p<0.01$(**) or $p<0.001$(***) when OA groups are compared to their normal- and sham-paired groups. Comparisons with normal and sham groups at 10, 20, and 45 days and normal and sham groups at 5 days are represented as

$p<0.01(^{\&\&})$ or $p<0.001(^{\&\&\&})$ for normal and $p<0.01(^{++})$ or $p<0.001(^{+++})$ for sham groups. Nine rats per experimental group were used (n=9).

Energy-dispersive X-ray spectroscopy

For EDX analyses, fixed condyles were rinsed twice with PBS, dehydrated in an ascending alcohol series to 100% ethanol, and then dried to critical point (Samdri 780, Tousimis, Rockville, MD, USA). Once dried, samples were coated with carbon (Vacuum Evaporator JEE-400, Jeol LTD, Tokyo, Japan) and analyzed for minerals using scanning electron microscopy coupled with energy-dispersive X-ray spectroscopy (JSM-6300S, Jeol LTD). This technique was performed to determine the proportion of calcium (Ca) and phosphorous (P) (the Ca/P ratio) as an indicator of mineralization in articular cartilage, and was only carried out in the superficial zone, in three different fields for each cartilage sample. The analysis was also performed in subchondral bone from normal healthy rats as a reference. Data are shown as mean ± standard deviation, and statistical significance is represented as $p<0.05(*)$, $p<0.01(**)$, or $p<0.001(***)$ when OA groups are compared to a healthy cartilage group. Three rats per experimental group were used (n=3).

Atomic force microscopy

Frozen condyles were cryosectioned to obtain 50-μm thick slices, which were mounted on gelatin-coated slides. Cartilage samples were thawed and dehydrated in an ascending alcohol series and then scanned to observe changes in the microstructure of the collagen fibrils during articular cartilage mineralization. The AFM (AutoProbe CP, ThermoMicroscopes, Veeco Instruments Inc. Plainview, NY, USA) was operated in contact and tapping mode, with a resonance frequency of 150-350 kHz. A scan rate of 1-2 kHz and a contact force of 10 Nn were used. Scanner actuators with lateral movements up to 5 μm and AFM tips of 2 nm curvature radius were used. Observations were only qualitative and were performed in the superficial zone of cartilage. Three rats per experimental group were used (n=3).

Statistical analysis

Statistical analyses were performed using the Graph Pad prism 5 program (Graph Pad Software Inc., San Diego, CA, USA). One-way ANOVA analysis with Tukey-Kramer multiple comparison tests and Dunnett's method was used to compare means among the experimental groups.

The correlation between the expression of Lxn and ALP in articular cartilage was determined by the Pearson correlation coefficient (r) with a 95% confidence interval.

Results

Lxn expression in articular cartilage during OA pathogenesis

As previously shown (Perez et al., 2010), Lxn is expressed in normal cartilage, and its levels increase with animal age (Fig. 1; normal and sham groups from 10-45 days vs. normal and sham groups at 5 days, $p<0.001$). Sham surgery did not affect Lxn expression levels, which were similar to those in normal cartilage (Fig. 1). Compared to normal and sham controls, Lxn expression was up-regulated in a time-dependent manner

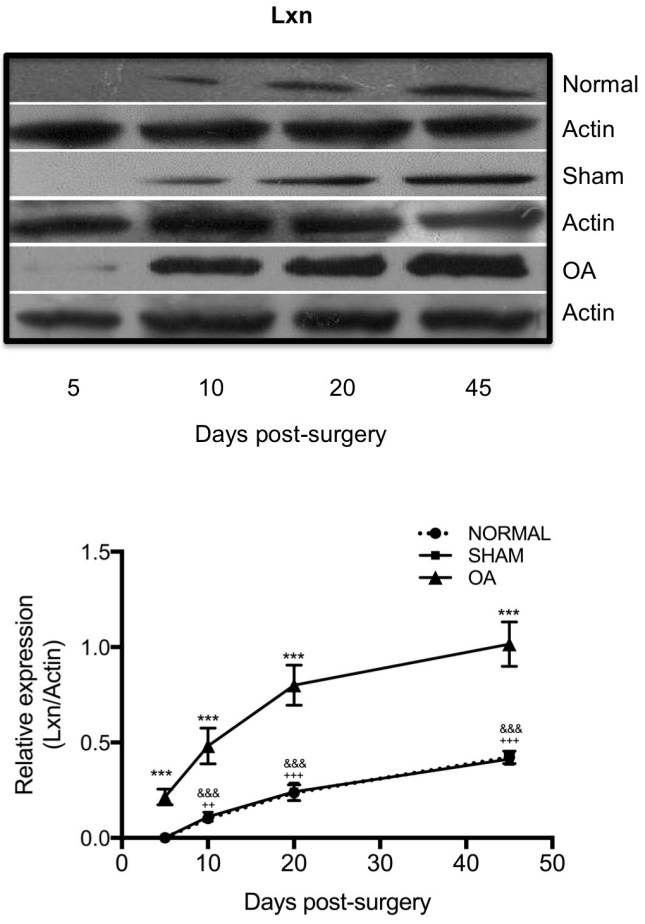

Fig. 1. Lxn levels in rat cartilage. On the indicated experimental days, rats were euthanized and articular cartilage was processed for Western blot. Data are the mean ratio of Lxn/actin ± standard deviation of normal, sham, and OA groups. Representative Western blot experiments are shown. Statistical significance is represented as $p<0.01(**)$ or $p<0.001(***)$ when OA values are compared to normal and sham groups. Comparisons between normal groups at 5 days and at 10, 20, and 45 days post-surgery and between sham groups at 5 days and at 10, 20, and 45 days are also represented as $p<0.001(\&\&\&)$ or $p<0.001(+++)$, respectively. Data from the following independent experiments: three normal (n=3), four sham (n=4) and seven OA groups (n=7).

in OA cartilage from the early stages of OA (Fig. 1; OA vs. normal and sham, p<0.001).

To determine the zone in OA cartilage where Lxn expression changed, we analyzed the three zones of the tissue. Immunofluorescence analysis showed that Lxn increased with age in normal and sham groups in all three zones of articular cartilage (Fig. 2; p<0.01 and p<0.05 in SZ at 20 days), mainly at 45 days post-surgery. However, in OA groups, Lxn expression was strongly up-regulated in the SZ from 5 to 45 days post-surgery (Fig. 2a,b; p<0.05 at 45 days, p<0.01at 10-20 days, and p<0.001 at 5 days) and in MZ and DZ only at 20 and 45 days post-surgery (Fig. 2a,c,d; p<0.05 at 45 days, and p<0.001 at 20 days). The basal expression of age-related Lxn in normal and sham groups detected by Western blot may be the sum of the partial expression in the three zones of cartilage.

As previously reported (Kadouchi et al., 2009; Parra-Torres et al., 2014), we observed Lxn expression in the nuclei of some MZ and DZ of OA chondrocytes. However, the role of Lxn in this subcellular location requires further studies.

ALP expression in osteoarthritic articular cartilage

ALP is considered to be a highly specific biomarker of bone-forming activity (Golub, 2009; Orimo, 2010), thus we evaluated its expression in articular cartilage as an indicator of cartilage mineralization. ALP is also expressed in normal cartilage, where its levels increase

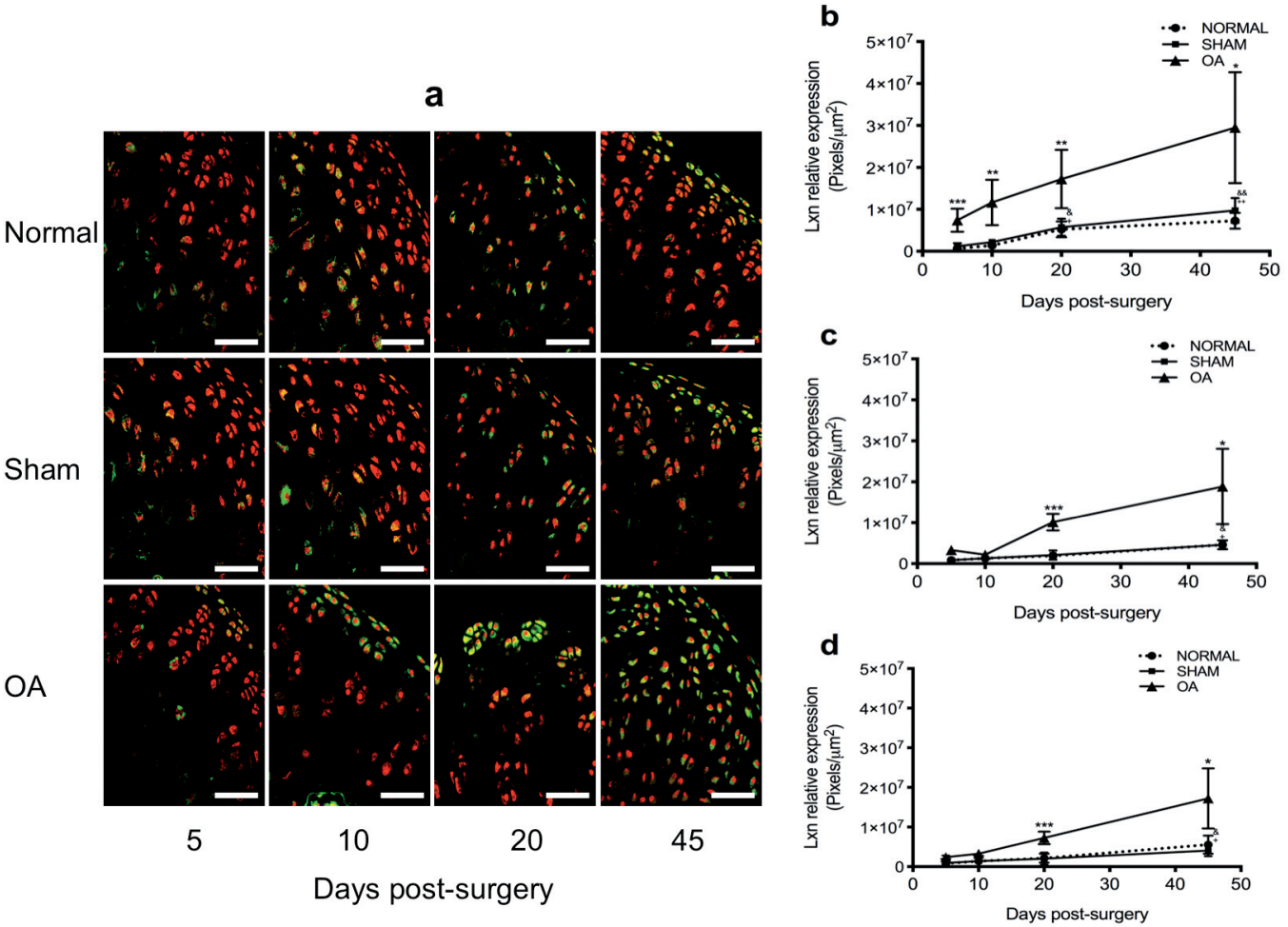

Fig. 2. Lxn expression and localization in articular cartilage. On the indicated experimental days, rats were euthanized and articular cartilage was processed for indirect immunofluorescence for Lxn. **a.** Representative immunofluorescence experiments for cartilage samples from normal, sham, and OA groups at 5, 10, 20 and 45 days are shown. Lxn was labeled with FITC (green), and nuclei were counterstained with propidium iodide (red). Scale bar: 75 μm. **b-d.** Graphical representation of Lxn expression in the cartilage zones. Data are mean relative Lxn expression ± standard deviation for normal, sham, and OA groups in the **b**) SZ, **c**) MZ, and **d**) DZ of cartilage. Statistical significance is represented as p<0.05(*), p<0.01(**), or p<0.001(***) when OA groups are compared to normal and sham groups. Comparisons between normal groups at 5 days and at 10-45 days post-surgery and between sham groups at 5 days and at 10-45 days post-surgery are also represented as p<0.05($^{\&}$) and p<0.01($^{\&\&}$) or p<0.05($^{+}$) and p<0.01($^{++}$), respectively. Data from 9 animals per experimental group (n=9).

with age (Fig. 3). Sham surgery did not affect ALP expression, which was similar to that in normal cartilage (Fig. 3). Compared to the basal expression observed in the control groups, ALP expression was up-regulated by a factor of approximately 2.4 at 5-45 days after surgery in OA groups (Fig. 3; OA vs normal and sham $p<0.001$, except at 45 days with $p<0.01$). The expression of ALP in OA cartilage correlated positively with the expression of Lxn, as showed by the Pearson´s coefficient ($r=0.9817$).

To determine if ALP expression was correlated with the zones of Lxn expression, we evaluated ALP activity in the different zones of articular cartilage. We found a progressive increase in the percentage of ALP-positive chondrocytes in the OA group when compared to the control groups (Fig. 4; OA vs normal and sham $p<0.001$ in the three zones, except at 45 days in the DZ, with $p<0.01$). In the control groups, ALP activity was only detected in chondrocytes from the DZ, in the proximity of subchondral bone (Fig. 4a,d). The increased basal expression of ALP found by Western blot in the normal and sham groups may be associated with the hypertrophic phenotype of chondrocytes in the DZ of cartilage. The analysis of the Pearson's coefficient showed: $r=0.9808$ in SZ, $r=0.9894$ in MZ, and $r=0.8668$ in DZ chondrocytes; supporting a strong positive correlation between the expression of Lxn and ALP in the whole OA articular cartilage.

Calcium minerals during OA pathogenesis

Determining the Ca/P ratio provides a sensitive measure of mineral bone turnover and may add to our understanding of changes in the mineralization of articular cartilage during OA progression. Our previous study (Martinez-Calleja et al., 2014) reported the deposition of calcium minerals (detected by alizarin red) in the SZ of cartilage during OA progression, thus we focused on this zone for determining the Ca/P ratio. The Ca/P ratio was low (more P than Ca) in healthy cartilage (0.38±0.065), showing no mineralization, but the Ca/P ratio increased during OA progression from 10 days post-surgery onwards, reaching the theoretical value for HA at 20 days post-surgery (1.69±0.2, Fig. 5). The ratio decreased at 45 days, to a value (0.90±0.12) close to OCP minerals, suggesting a dynamic turnover in cartilage mineralization. These findings support that mineralization also occurs in the SZ of OA cartilage. As a reference, we determined that the Ca/P ratio in the subchondral bone of healthy rats was 1.1±0.067, very close to that reported for BCP minerals.

AFM has been used to evaluate the organization and ultrastructure of mineralized collagen fibrils [reviewed in (Georgiadis et al., 2016). With AFM, the typical periodic banding pattern of collagen fibrils is more evident in demineralized than in mineralized tissue, as minerals are deposited on and along collagen fibrils (Sasaki et al., 2002). We thus used AFM to evaluate the organization of collagen fibrils in cartilage during the progression of OA. In normal, healthy cartilage, collagen fibrils showed a typical periodic banding pattern (Fig. 6, black arrows). A similar banding pattern was observed in the OA cartilage at 5 days post surgery (Fig. 6, black arrows) suggesting absence of minerals in this OA stage. In contrast, at 10, 20, and 45 days after surgery, the network of collagen fibers in the OA cartilage showed changes in its structure (mainly at 20 and 45 days post-surgery)—including breakdown (white pentagons) and loss of collagen banding pattern (black arrowheads, Fig. 8)—suggesting enzymatic degradation and/or the deposition of minerals on collagen fibrils.

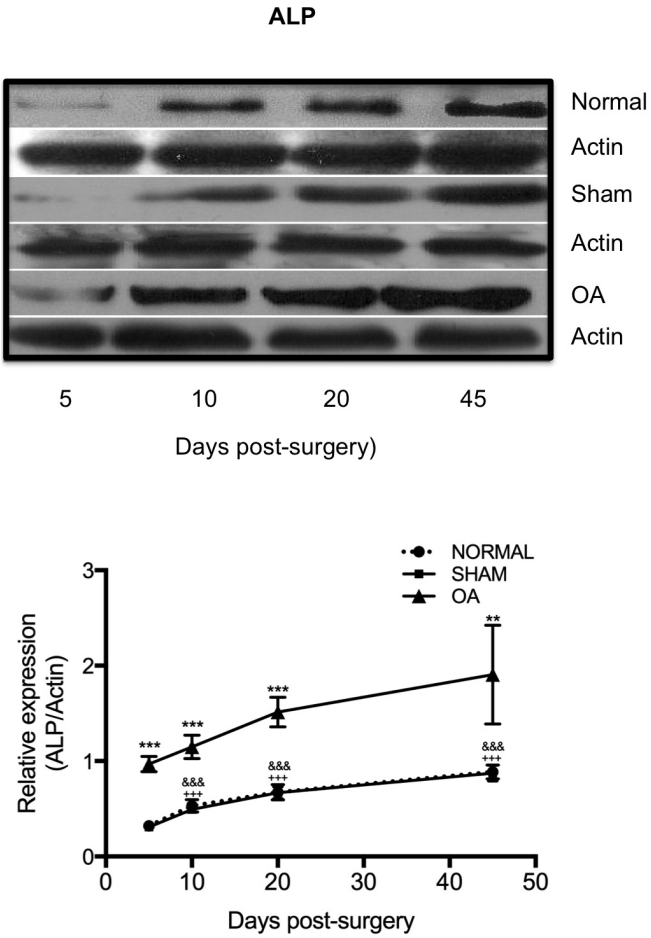

Fig. 3. ALP levels in rat cartilage. On the indicated experimental days, rats were euthanized and articular cartilage was processed for Western blot. Data are the mean ratio of ALP/actin ± standard deviation in normal, sham, and OA groups. Representative Western blot experiments are shown. Statistical significance is represented as $p<0.01$(**) or $p<0.001$(***) when OA values are compared to normal and sham groups. Comparisons between normal groups at 5 days and at 10-45 days post-surgery and between sham groups at 5 days and 10-45 days post-surgery are also represented as $p<0.001$($^{\&\&\&}$) or $p<0.001$($^{+++}$), respectively. Data from the following independent experiments: three normal and sham (n=3) and four OA groups (n=4).

Discussion

The molecules involved in the mineralization of articular cartilage during OA pathogenesis have not been completely identified, but hypertrophic-related molecules are of great interest since chondrocytes in OA cartilage share features with endochondral ossification, such as hypertrophy and the capability to mineralize the matrix (Fuerst et al., 2009). As Lxn has been involved in hypertrophic chondrocyte differentiation and bone formation (Kadouchi et al., 2009), we look for new evidence to correlate its expression with signs of articular cartilage mineralization in an OA rat model. Our results show that Lxn is up-regulated in a time-dependent manner during OA progression. Expression levels were found to be correlated positively with the expression and activity of the mineralization marker ALP that together with changes in the Ca/P ratio and alterations in the structure of collagen fibrils, suggest that Lxn could be involved in the mineralization of articular cartilage. Certainly our study is descriptive and the precise molecular mechanism by which Lxn modulates cartilage mineralization requires further and detailed research.

Cartilage mineralization has not been studied in an animal model with the targeted deletion of the Lxn gene. However, gene profiling of Lxn-null hematopoietic stem cells (HSCs) has shown altered expression of genes

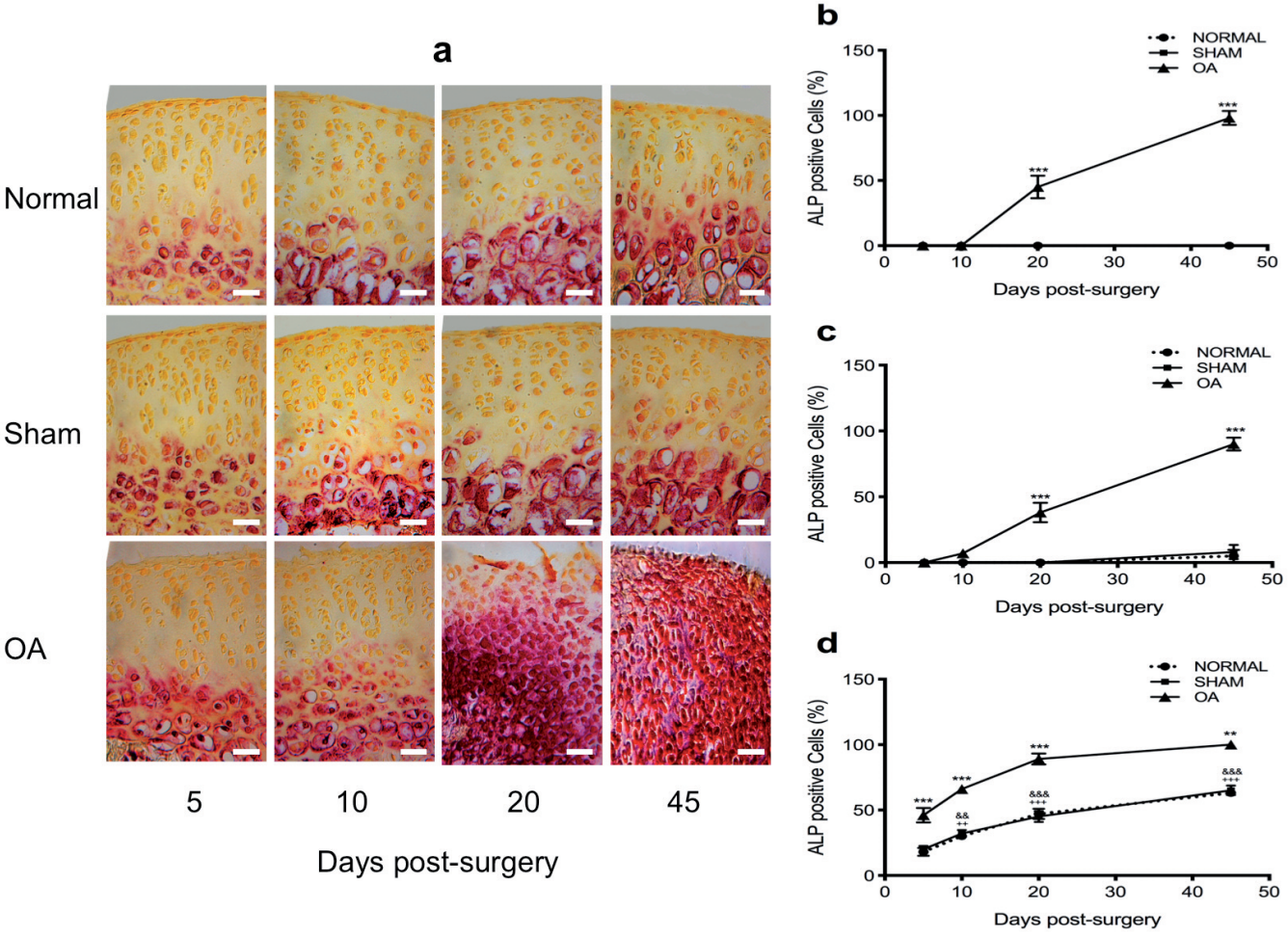

Fig. 4. ALP activity in articular cartilage. On the indicated experimental days, rats were euthanized and articular cartilage was processed for in situ ALP activity. **a.** Representative histochemical experiments for cartilage samples from normal sham and OA groups at 5, 10, 20, and 45 days are shown. Chondrocytes positive for ALP activity show a red/purple color. Scale bar: 50 μm. **b-d.** Graphical representation of ALP activity in the cartilage zones. Data are the mean number of positive cells for ALP activity ± standard deviation for normal, sham, and OA groups in the **b**) SZ, **c**) MZ, and **d**) DZ of cartilage. Statistical significance is represented as $p<0.01$(**) or $p<0.001$(***) when OA groups are compared to normal and sham groups. Comparisons between normal groups at 5 days and at 10-45 days post-surgery and between sham groups at 5 days and at 10-45 days post-surgery are also represented as $p<0.01$($^{\&\&}$) and $p<0.001$($^{\&\&\&}$) (for normal) or $p<0.01$($^{++}$) and $p<0.001$($^{+++}$), respectively. Data from 9 animals per experimental group (n=9).

associated with cell-matrix and cell-cell interactions (Liu et al., 2017). Among these genes, Thrombospondin 1 (THBS1) is a downstream target which inhibits osteoblast differentiation and its knockdown results in increased ALP activity and accelerated mineralization (Hankenson et al., 2010). THSB1 is expressed in the MZ chondrocytes in normal cartilage, where it is up-regulated in early OA but decreased in severe OA (Pfander et al., 2000), pointing to a role as an inhibitor of hypertrophic chondrocyte differentiation. However, the link between Lxn, THBS1, and mineralization in our traumatic OA model must now be demonstrated experimentally, as we found increased Lxn expression that should have been associated with a decrease in mineralization, which did not occur. This can only be explained if the regulation of the expression of Lxn downstream targets is lost during OA pathogenesis to drive the phenotype of chondrocytes to hypertrophic. Thus, in healthy cartilage the expression of Lxn that we detected in chondrocytes cannot be associated with OA progression since a balance between catabolic/anabolic molecules must exist to maintain the integrity of the healthy cartilage (Rojas-Ortega et al., 2015). Interestingly, mineral deposition was only detected after the Lxn expression was up-regulated (5 days after OA induction, Figs. 1, 2), indicating that its activity precedes and remains during the pathological cartilage mineralization. If Lxn participates in the termination of mineral deposition, as its homologous OCX-32 in the formation of the eggshell (Hincke et al., 2003), it is not known and should be investigated. We cannot discard the CPA inhibitory activity of Lxn to regulate the function of proteins involved in the

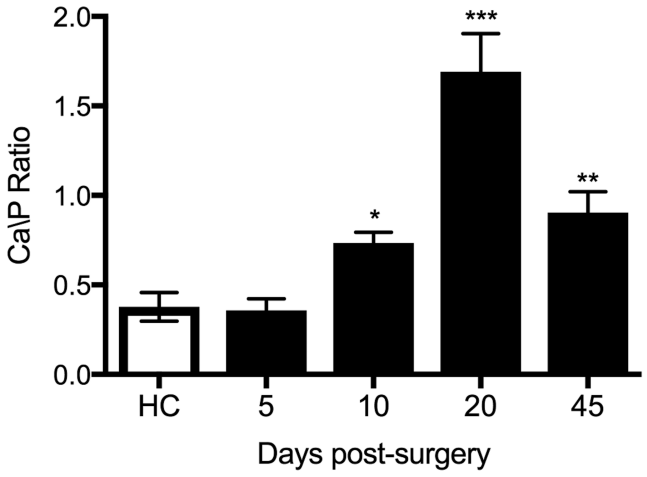

Fig. 5. Ca/P ratio during the progression of OA. On the indicated experimental days, rats were euthanized and articular cartilage was processed for EDX analysis. Data are shown as the mean Ca/P ratio ± standard deviation, and statistical significance is represented as p<0.05(*), p<0.01(**), or p<0.001(***) when OA groups are compared to the healthy cartilage group. Data from 3 animals per experimental group (n=3).

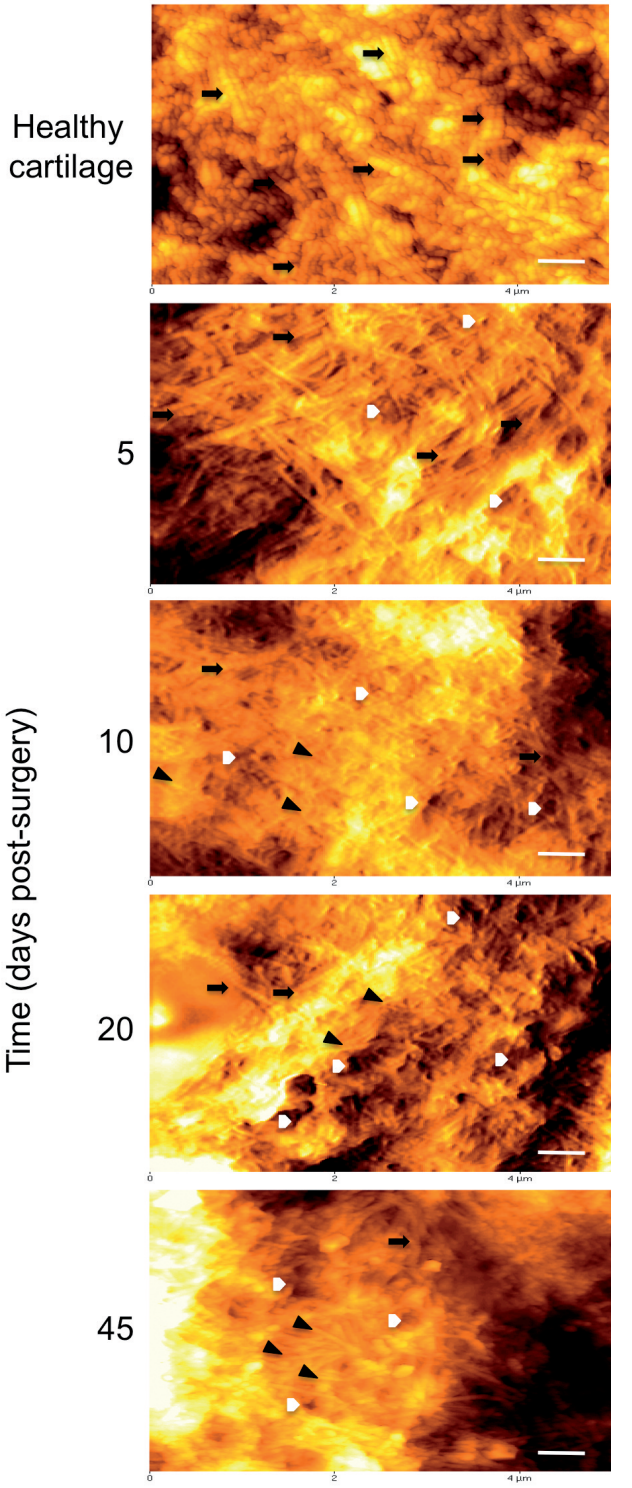

Fig. 6. Structural changes in collagen fibers during OA pathogenesis. On the indicated experimental days, rats were euthanized and articular cartilage was processed for AFM observations. The collagen fibrils were observed as triple bands (black arrows), which are characteristic of healthy cartilage. In OA cartilage at 10, 20 and 45 days post-surgery, the collagen fibrils showed alterations in their organization and were more lax due to the loss of banding pattern (black arrowheads) and breakdowns (white pentagons). Scale bar: 0.5 μm.

differentiation/mineralization of chondrocytes.

Although in this study we did not look directly for calcium minerals in the articular cartilage, we used EDX and AFM analysis as approaches to determine their presence. The increase in the Ca/P ratio at 20 days of OA induction (Fig. 5) was very close to that reported for HA which is 1.67 (Fuerst et al., 2010) while the increased Ca/P ratio at 10 and 45 days (0.7 and 0.9, respectively) are very close to OCP minerals that are precursor phases of HA. As nucleation of apatite is controlled by the hydrolysis of transient mineral phases (TCP and OCP) (Fuerst et al., 2010), our results support the hypothesis of a dynamic turnover of calcium crystals in the articular cartilage during OA pathogenesis. During bone formation, collagen fibers serve as a scaffold for the first mineral deposits (Golub, 2009), thus once they are mineralized, collagen fibers are no longer visible by AFM. Something similar may occur in articular cartilage, where the increases we found in the Ca/P ratio suggest calcium deposits in the SZ chondrocytes. Moreover, the changes we found in the ECM of OA cartilage can also be associated with the loss of the collagen periodic banding pattern due to enzymatic degradation by MMPs, a molecular process widely demonstrated in OA pathogenesis (Cruz et al., 2013). Further studies are required, then, to determine if the collagen fibers act as scaffolds for the growth of crystals in articular cartilage as has been described for bone formation (Golub, 2009). Certainly, transmission electron microscopy studies are needed to determine the presence of typical vesicles emerging from chondrocytes, and spectroscopic studies are required to unequivocally establish the presence of HA or any other BCP minerals in the cartilage.

Our results show mineral deposition in articular cartilage of post-traumatic OA joints and points out that Lxn is involved in mineralization during OA onset. A better understanding of the molecules and mechanism associated with abnormal mineralization of articular cartilage at early stages of the disease may lead to new therapeutic approaches to prevent the degenerative process.

Acknowledgements. We are grateful to Dr. Angel Guillen-Cervantes, Biol. Lizbeth Salazar-Villatoro, and Ivan J. Galván-Mendoza for their technical support.

Conflict of interest statement. The authors declare no conflicts of interest.

Funding information. This work was supported by the Consejo Nacional de Ciencia y Tecnología [grant number 168328 to JBK]. The publication fee for this paper was paid by MAVL with personal funds.

References

Aagaard A., Listwan P., Cowieson N., Huber T., Ravasi T., Wells C.A., Flanagan J.U., Kellie S., Hume D.A., Kobe B. and Martin J.L. (2005). An inflammatory role for the mammalian carboxypeptidase inhibitor latexin: Relationship to cystatins and the tumor suppressor tig1. Structure 13, 309-317.

Arimatsu Y., Nihonmatsu I. and Hatanaka Y. (2009). Localization of latexin-immunoreactive neurons in the adult cat cerebral cortex and claustrum/endopiriform formation. Neuroscience 162, 1398-1410.

Balint E., Lapointe D., Drissi H., van der Meijden C., Young D.W., van Wijnen A.J., Stein J.L., Stein G.S. and Lian J.B. (2003). Phenotype discovery by gene expression profiling: Mapping of biological processes linked to bmp-2-mediated osteoblast differentiation. J. Cell. Biochem. 89, 401-426.

Corr E.M., Cunningham C.C., Helbert L., McCarthy G.M. and Dunne A. (2017). Osteoarthritis-associated basic calcium phosphate crystals activate membrane proximal kinases in human innate immune cells. Arthritis Res. Ther. 19, 23.

Cruz R., Miranda-Sanchez M., Solis-Garcia D. and Kouri J. (2013). Recent patents on metalloproteinases as biomarkers in osteoarthritis diagnosis and treatment. Rec. Pat. Biomark. 4, 1-10.

Frallonardo P., Oliviero F., Peruzzo L., Tauro L., Scanu A., Galozzi P., Ramonda R. and Punzi L. (2016). Detection of calcium crystals in knee osteoarthritis synovial fluid: A comparison between polarized light and scanning electron microscopy. J. Clin. Rheumatol. 22, 369-371.

Fuerst M. (2014). Chondrocalcinosis. Clinical impact of intra-articular calcium phosphate crystals. Z. Rheumatol. 73, 415-419 (in German).

Fuerst M., Lammers L., Schafer F., Niggemeyer O., Steinhagen J., Lohmann C.H. and Ruther W. (2010). Investigation of calcium crystals in oa knees. Rheumatol. Int. 30, 623-631.

Fuerst M., Bertrand J., Lammers L., Dreier R., Echtermeyer F., Nitschke Y., Rutsch F., Schafer F.K., Niggemeyer O., Steinhagen J., Lohmann C.H., Pap T. and Ruther W. (2009). Calcification of articular cartilage in human osteoarthritis. Arthritis Rheum. 60, 2694-2703.

Georgiadis M., Muller R. and Schneider P. (2016). Techniques to assess bone ultrastructure organization: Orientation and arrangement of mineralized collagen fibrils. J. R. Soc. Interface 13.

Goldring M.B. and Goldring S.R. (2010). Articular cartilage and subchondral bone in the pathogenesis of osteoarthritis. Ann. N. Y. Acad. Sci. 1192, 230-237.

Golub E.E. (2009). Role of matrix vesicles in biomineralization. Biochim. Biophys. Acta 1790, 1592-1598.

Hankenson K.D., Sweetwyne M.T., Shitaye H. and Posey K.L. (2010). Thrombospondins and novel TSR-containing proteins, R-spondins, regulate bone formation and remodeling. Curr. Osteoporos. Rep. 8, 68-76.

Hincke M.T., Gautron J., Mann K., Panheleux M., McKee M.D., Bain M., Solomon S.E. and Nys Y. (2003). Purification of ovocalyxin-32, a novel chicken eggshell matrix protein. Connect. Tissue Res. 44 (Suppl 1), 16-19.

Kadouchi I., Sakamoto K., Tangjiao L., Murakami T., Kobayashi E., Hoshino Y. and Yamaguchi A. (2009). Latexin is involved in bone morphogenetic protein-2-induced chondrocyte differentiation. Biochem. Biophys. Res. Commun. 378, 600-604.

Kouri J.B., Aguilera J.M., Reyes J., Lozoya K.A. and Gonzalez S. (2000). Apoptotic chondrocytes from osteoarthrotic human articular cartilage and abnormal calcification of subchondral bone. J. Rheumatol. 27, 1005-1019.

Liang Y. and Van Zant G. (2008). Aging stem cells, latexin, and longevity. Exp. Cell Res. 314, 1962-1972.

Liu Y., Zhang C., Li Z., Wang C., Jia J., Gao T., Hildebrandt G., Zhou D., Bondada S., Ji P., St Clair D., Liu J., Zhan C., Geiger H., Wang

S. and Liang Y. (2017). Latexin inactivation enhances survival and long-term engraftment of hematopoietic stem cells and expands the entire hematopoietic system in mice. Stem Cell Reports 8, 991-1004.

Lozoya K.A. and Flores J.B. (2000). A novel rat osteoarthrosis model to assess apoptosis and matrix degradation. Pathol. Res. Pract. 196, 729-745.

Martinez-Calleja A., Velasquillo C., Vega-Lopez M., Arellano-Jimenez M.J., Tsutsumi-Fujiyoshi V.K., Mondragon-Flores R. and Kouri-Flores J.B. (2014). Osteopontin expression and localization of Ca^{++} deposits in early stages of osteoarthritis in a rat model. Histol. Histopathol. 29, 925-933.

Ni Q.F., Tian Y., Kong L.L., Lu Y.T., Ding W.Z. and Kong L.B. (2014). Latexin exhibits tumor suppressor potential in hepatocellular carcinoma. Oncol. Rep. 31, 1364-1372.

Orimo H. (2010). The mechanism of mineralization and the role of alkaline phosphatase in health and disease. J. Nippon Med. Sch. 77, 4-12.

Parra-Torres N.M., Cazares-Raga F.E. and Kouri J.B. (2014). Proteomic analysis of rat cartilage: The identification of differentially expressed proteins in the early stages of osteoarthritis. Proteome Sci. 12, 55.

Perez E., Gallegos J.L., Cortes L., Calderon K.G., Luna J.C., Cazares F.E., Velasquillo M.C., Kouri J.B. and Hernandez F.C. (2010). Identification of latexin by a proteomic analysis in rat normal articular cartilage. Proteome Sci. 8, 27.

Pfander D., Cramer T., Deuerling D., Weseloh G. and Swoboda B. (2000). Expression of thrombospondin-1 and its receptor CD36 in human osteoarthritic cartilage. Ann. Rheum. Dis. 59, 448-454.

Rojas-Ortega M., Cruz R., Vega-Lopez M.A., Cabrera-Gonzalez M., Hernandez-Hernandez J.M., Lavalle-Montalvo C. and Kouri J.B. (2015). Exercise modulates the expression of il-1beta and il-10 in the articular cartilage of normal and osteoarthritis-induced rats. Pathol. Res. Pract. 211, 435-443.

Sasaki N., Tagami A., Goto T., Taniguchi M., Nakata M. and Hikichi K. (2002). Atomic force microscopic studies on the structure of bovine femoral cortical bone at the collagen fibril-mineral level. J. Mater. Sci. Mater. Med. 13, 333-337.

Velasquillo C., Garciadiego-Cazares D., Almonte M., Bustamante M., Ibarra C., Kouri J.B. and Chimal-Monroy J. (2007). Expression of MIG-6, WNT-9a, and WNT-7b during osteoarthritis. Ann. N. Y. Acad. Sci. 1117, 175-180.

Yamaguchi R., Yamamoto T., Motomura G., Ikemura S., Iwasaki K., Zhao G., Doi T. and Iwamoto Y. (2014). Bone and cartilage metabolism markers in synovial fluid of the hip joint with secondary osteoarthritis. Rheumatology (Oxford) 53, 2191-2195.

Yu Y.Y., Lieu S., Lu C. and Colnot C. (2010). Bone morphogenetic protein 2 stimulates endochondral ossification by regulating periosteal cell fate during bone repair. Bone 47, 65-73.

Accepted July 17, 2019